

# Extreme escalation of heat failure rates in ectotherms with global warming

<https://doi.org/10.1038/s41586-022-05334-4>

Received: 14 December 2021

Accepted: 9 September 2022

Published online: 26 October 2022

 Check for updates

Lisa Bjerregaard Jørgensen<sup>1</sup>, Michael Ørsted<sup>1</sup>, Hans Malte<sup>1</sup>, Tobias Wang<sup>1</sup> & Johannes Overgaard<sup>1</sup> 

Temperature affects the rate of all biochemical processes in ectotherms<sup>1,2</sup> and is therefore critical for determining their current and future distribution under global climate change<sup>3–5</sup>. Here we show that the rate of biological processes maintaining growth, homeostasis and ageing in the permissive temperature range increases by 7% per degree Celsius (median activation energy  $E_a = 0.48$  eV from 1,351 rates across 314 species). By contrast, the processes underlying heat failure rate within the stressful temperature range are extremely temperature sensitive, such that heat failure increases by more than 100% per degree Celsius across a broad range of taxa (median  $E_a = 6.13$  eV from 123 rates across 112 species). The extreme thermal sensitivity of heat failure rates implies that the projected increase in the frequency and intensity of heatwaves can exacerbate heat mortality for many ectothermic species with severe and disproportionate consequences. Combining the extreme thermal sensitivities with projected increases in maximum temperatures globally<sup>6</sup>, we predict that moderate warming scenarios can increase heat failure rates by 774% (terrestrial) and 180% (aquatic) by 2100. This finding suggests that we are likely to underestimate the potential impact of even a modest global warming scenario.

Temperature has a profound influence on processes at all levels of biological organization, ranging from the simple catalytic rates of enzymes to the complex biological interactions that underlie metabolism, growth and reproduction of ectothermic animals<sup>1,2</sup>. The interactions between multiple temperature-sensitive biological rates ultimately shape thermal performance and determine the thermal limits for life and death in ectotherms<sup>1,7,8</sup>. Accordingly, thermal tolerance limits are robust predictors of the geographical distribution of ectothermic animals<sup>3,9,10</sup>, and climate change beyond tolerance limits can explain their current redistributions<sup>4,11</sup>.

## Thermal sensitivity of life and death

Temperature effects on biological rates are often described using  $Q_{10}$  (the factorial change in biological rate resulting from a 10 °C increase) but are more appropriately expressed by the Arrhenius activation energy  $E_a$  (ref. <sup>2</sup>). When rates are measured within permissive temperatures, defined as temperatures that allow for long-term survival,  $E_a$  typically ranges from 0.5 to 0.8 eV (equivalent to  $Q_{10} \approx 2–3$ ) corresponding to a 7–12% rate increase per degree Celsius<sup>12–14</sup>. The consequences of global warming on the rate of energy metabolism in ectotherms are already implemented in contemporary analyses of ecosystems and agriculture<sup>14–16</sup>. However, temperature also affects biological rate functions at stressful temperatures, defined here as the temperature range causing acute heat injury and mortality. The temperature sensitivity of these processes is much more potent in ectothermic animals<sup>17–19</sup> but has received little attention in the context of global warming.

The disparate temperature sensitivities in the permissive and stressful temperature range can be exemplified through a combined analysis

of temperature effects on the population growth capacity<sup>20</sup> and lifespan<sup>18</sup> of adult fruit flies (*Drosophila subobscura*; Fig. 1a). Within the permissive temperature range for this species (3–28 °C), warming increases the rates of biological processes in a manner that initially enhances fitness, that is, the product of egg laying rate, developmental viability and developmental speed<sup>20</sup>. However, as temperature increases further, the balance between catabolic and anabolic rates shifts and net fitness decreases<sup>1,7,8,21</sup> even if it remains positive. This declining fitness occurs even though many biological rates—such as feeding rate, heart rate, metabolic rate and ageing/mortality rate—continue to increase with the same thermal sensitivity throughout the permissive range<sup>22</sup>. Accordingly, when lifespan is analysed across the permissive temperature range, the increased rates of biological activities coincide with an acceleration of senescence and ageing<sup>23,24</sup>. In this example, the thermal sensitivity,  $Q_{10} = 2.5$  for ageing/mortality rate (1/lifespan) (Fig. 1a), corresponds to an Arrhenius activation energy  $E_a$  of 0.66 eV (Fig. 1b). Similar moderate thermal sensitivities of ageing/mortality rate (1/lifespan) at permissive temperatures have been documented in a variety of ectothermic species ( $E_a = 0.56 \pm 1$  eV (mean ± s.d.) across 97 field and laboratory populations<sup>24</sup>).

There is a substantial shift in the influence of temperature on lifespan above a critical temperature  $T_c$ , defined as the temperature or narrow temperature zone that separates the permissive and stressful temperature range (Fig. 1). Although  $T_c$  is rarely parametrized experimentally (see the discussion in ref. <sup>22</sup>), it represents a temperature at which biological processes dictating the ‘rate of death’ become dominant over those determining the ‘rate of life’. Heat failure rate above  $T_c$  is also calculated as 1/lifespan, and the Arrhenius breakpoint<sup>1,2</sup> at  $T_c$  indicates

<sup>1</sup>Section for Zoophysiology, Department of Biology, Aarhus University, Aarhus, Denmark. <sup>✉</sup>e-mail: johannes.overgaard@bio.au.dk

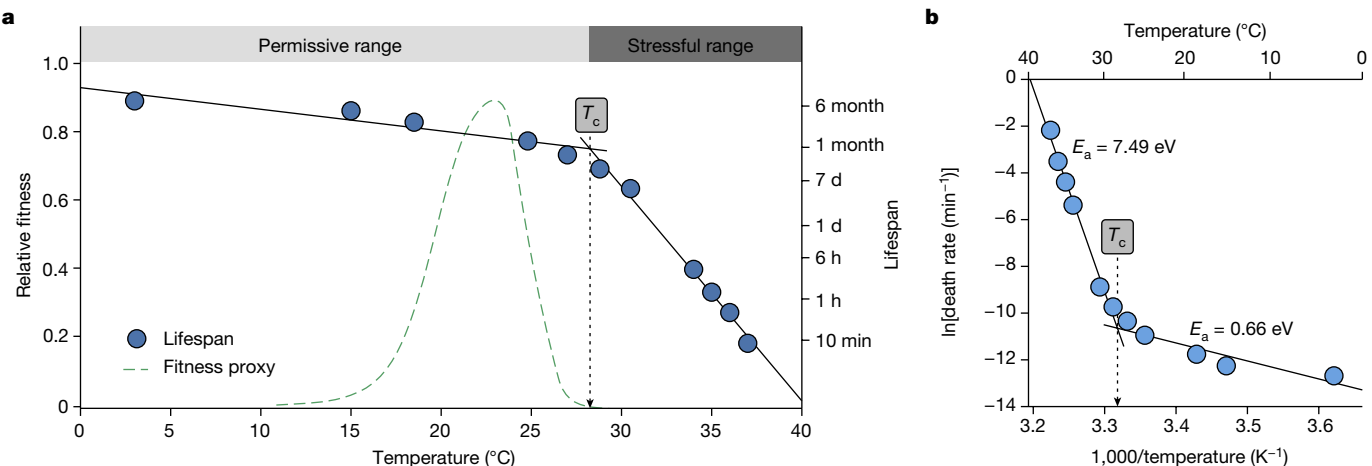


**Fig. 1 | Disparate temperature sensitivities for the lifespan of an ectotherm reveal permissive and stressful temperature domains.** **a**, Lifespan of adult fruit flies (*D. subobscura*) depicted on a log<sub>10</sub> scale to indicate the exponential relationship between temperature and lifespan (right y axis; data are from ref.<sup>18</sup>). The critical temperature ( $T_c$ ) indicates the transition at which the temperature effect on lifespan (slope) diverts from that of biological processes in the permissive temperature range to become extremely high in the stressful temperature range. A thermal performance curve for reproductive fitness in

*D. subobscura* in the permissive temperature range illustrates that this is the range of temperatures that permits completion of the life cycle (dashed green curve on the left y axis; data are from ref.<sup>20</sup>). **b**, Temperature-specific death rates calculated as 1/lifespan from **a** were analysed in an Arrhenius plot. Activation energies  $E_a$  are indicated for the permissive ( $E_a = 0.66$  eV) and stressful ( $E_a = 7.49$  eV) temperature ranges separated at a breakpoint temperature  $T_c$  (28.2 °C) found using Davies' test for a change in slope ( $P < 0.001$ ).

that the heat failure rate is dictated by different biological processes that are extremely sensitive to temperature ( $Q_{10} = 8,726$  (Fig. 1a) and  $E_a = 7.49$  eV (Fig. 1b)). For *D. subobscura*, heat death occurs after 6 h at 33 °C, while 4 °C further warming reduces its lifespan to less than 10 min (Fig. 1a). Similar extreme thermal sensitivities of heat failure have been described in thermal death time curves for many other ectotherms<sup>19,25,26</sup>.

### Analysis of activation energies

The fundamentally different thermal sensitivities for processes associated with life (permissive range) and death (stressful range) are not unique for *D. subobscura* (Fig. 1). Data compiled on 1,351 rates across different temperatures from 314 species show that the  $E_a$  of biological processes within the permissive temperature range (median  $E_a = 0.48$  eV; interquartile range (IQR) = 0.28–0.71 eV; Fig. 2a,b) are indeed consistent with textbook values of  $E_a \approx 0.5$ –0.8 eV ( $Q_{10} \approx 2$ –3) for most ectothermic animals<sup>12–14</sup>. As previously discussed<sup>13,14</sup>, these thermal sensitivities mirror most biological processes, including enzyme catalytic rates and integrated biological functions, such as feeding rate and metabolic rate (Fig. 2a,b and Extended Data Table 1). However, note that the integrated effect of many underlying biological rates causes a decline in ‘fitness’ in the warmer part of the permissive temperature range. As a consequence, the population growth rate (fitness) is associated with  $E_a < 0$  or  $Q_{10} < 1$  at the warmest permissive temperatures (Box 1) even though many underlying biological rates continue to increase after fitness has peaked at the optimal temperature ( $T_{opt}$ )<sup>22</sup>.

In contrast to the modest temperature sensitivity of biological rates in the permissive temperature range, the rate of heat failure is extraordinarily temperature sensitive in the stressful temperature range (Fig. 2c,d). We compiled data on the thermal sensitivity of heat failure for 112 species (123 datasets in total) with the criteria that time to heat failure was measured at three or more constant test temperatures. Heat failure rates ( $\text{min}^{-1}$ ) were calculated as 1/time to heat failure (min) and the activation energy was subsequently calculated using an Arrhenius analysis (Fig. 2c). Heat failure rate has extreme thermal sensitivity across all of the ectotherms examined (Fig. 2d) with a median  $E_a = 6.13$  eV (IQR = 4.42–8.82 eV) corresponding to a median  $Q_{10} > 1,500$  and more than a doubling of heat failure rate per 1 °C of warming (median increase = 110%, IQR = 71–190%). The median duration of the heat failure experiments was 125 min

(IQR = 31.5–422 min), with 122 out of 123 median durations less than 2.5 days, emphasizing that our estimates of heat failure rate are relevant for the acute heat exposures experienced during daily fluctuations and heatwaves<sup>25</sup>. All five ectothermic groups (fishes, crustaceans, molluscs, amphibians and insects) have a median  $E_a > 4.63$  eV, but vertebrates are particularly sensitive to warming (median  $E_a = 10.06$  eV and 10.30 eV for fishes and amphibians, respectively). This analysis also shows that  $E_a$  is high for both terrestrial ( $E_a = 5.53$  eV; IQR = 4.13–6.42 eV) and aquatic species ( $E_a = 6.69$  eV; IQR = 4.61–10.38 eV). Given the extraordinarily high thermal sensitivities in all taxonomic groups, we suggest that the extreme thermal sensitivity of heat failure rate is a general characteristic of all ectothermic animals.

The physiological causes of heat death in ectotherms are still poorly understood, but have been associated with protein denaturation, oxygen limitation, loss of cellular excitability and membrane dysfunction<sup>2,7,8,12,21,27</sup>. It is also unclear why the rates of these processes accelerate so substantially at extreme temperatures above  $T_c$ . Nevertheless, it is likely the same physiological dysfunctions that underlie chronic (hours) and acute (minutes) heat stress as exposure to different temperatures above  $T_c$  is additive in both fish<sup>19</sup> and insects<sup>25</sup>. Furthermore, the absence of Arrhenius breakpoints<sup>2</sup> above  $T_c$  suggests that heat failure is caused by a common heat stress syndrome that accelerates in intensity with an extreme thermal sensitivity. Importantly, many underlying biological rates typically begin to decrease within the stressful temperature range. Thus, metabolic rate, movement rate and heart rate, which typically increase throughout the permissive range<sup>22</sup>, will eventually decline as temperatures become acutely stressful. The thermal sensitivity of this rate decline in the stressful temperature range is typically higher than the thermal sensitivity of the rate increase occurring in the permissive temperature range<sup>13,22,28,29</sup>. However, it remains difficult to pinpoint whether the extreme increase in death rate at stressful temperatures substantially limits heart rate, metabolic rate and movement rate or vice versa, as the causalities of the physiological heat stress syndrome are currently poorly understood<sup>2,8,22,27</sup>.

### Implications of global warming

In their active season, ectothermic animals are mostly confined to habitats with permissive temperatures that enable reproduction and

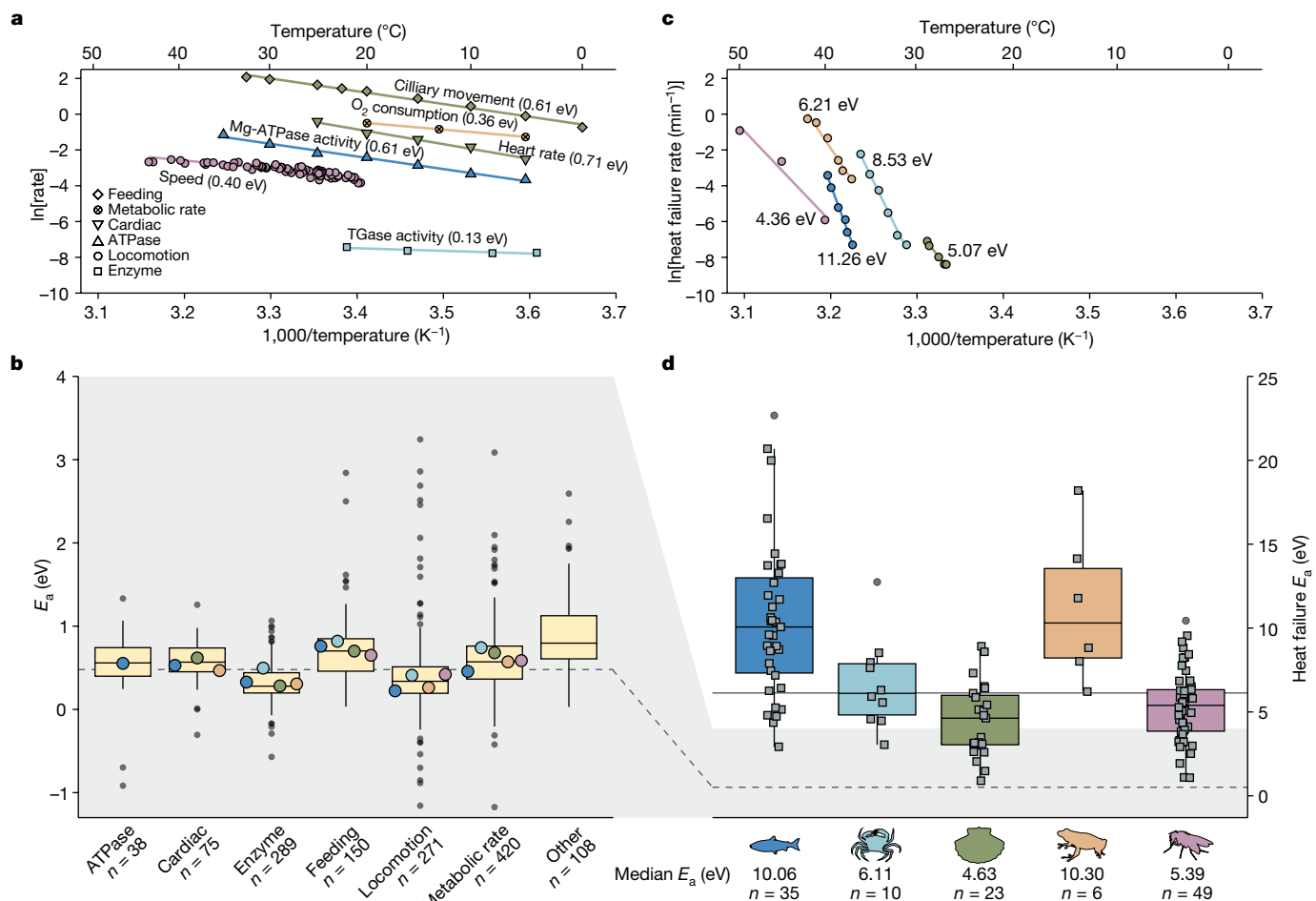


**Fig. 2 | Thermal sensitivity of biological processes sustaining life in the permissive temperature range or causing heat death in the stressful temperature range.** Data are organized in five ectotherm groups (fishes, crustaceans, molluscs, amphibians and insects) for which the most published data exist. **a**, Six representative examples of temperature sensitivity of biological processes measured within the permissive (non-stressful) temperature range (colour refers to the animal group and symbols to the trait; details are provided in Extended Data Table 1). **b**, Data from 1,351 literature estimates of  $E_a$  measured in the permissive temperature range from 314 species grouped by biological process. Coloured points represent averages in cases in which  $n \geq 8$  for that animal group. Data from ectotherms not belonging to the five groups are also included in the box plots. The dashed line indicates the

global median ( $E_a = 0.48 \text{ eV}$ , corresponding to  $Q_{10} = 1.9$ ). The box plots summarize each categorized biological process; the centre line shows the median, the box limits represent the first and third quartiles, the whiskers extend to  $1.5 \times \text{IQR}$  and the grey points show outliers. **c**, Representative examples of heat failure rates and their activation energy ( $E_a$ ) measured in the stressful temperature range (the same or closely related species as in **a**). **d**, Activation energies of heat failure rate organized by ectothermic group with all 123  $E_a$  values shown (squares, from 112 unique species). The full line indicates the global median ( $E_a = 6.13 \text{ eV}$ , corresponding to  $Q_{10} > 1,500$ ). For reference to **b**, the grey area denotes the  $E_a$  range  $-1.3\text{--}4 \text{ eV}$ , and the dashed line indicates the median  $E_a$  for processes in the permissive range.

population growth<sup>1,2,7</sup>. Even so, ectotherms may experience stressful temperatures (exceeding  $T_c$ ) during heatwaves or diurnal/seasonal temperature extremes. Tolerance to extremes is therefore an important determinant of species distributions<sup>3,9</sup>, and thermal tolerance limits ( $CT_{\min}$  and  $CT_{\max}$ ) often correlate stronger with distribution than the thermal optimum for population growth ( $T_{opt}$ ), a performance measure within the permissive temperature range<sup>20,30</sup>.

The severity of stressful temperatures depends on both the intensity (that is, the actual temperature) and the duration of the exposure<sup>17,19,22,25,26</sup>. The considerable thermal sensitivity of ectothermic heat failure rates more than doubles heat stress with every degree Celsius of warming. Accordingly, even modest increases in maximal exposure temperature—for example, as a result of moderate global warming—can substantially exacerbate the severity of heat injury. The potential magnitude of this problem was assessed by associating the median  $E_a$  for terrestrial and aquatic ectotherms with projected increases in maximum temperature for three IPCC warming

scenarios (Fig. 3a and Extended Data Table 2). This analysis represents a worst-case scenario based on the assumption that species under current climate conditions experience temperatures equal to or above  $T_c$  on the warmest days within their distribution range. Terrestrial environments are projected to warm considerably more than aquatic environments<sup>6</sup> (Fig. 3 and Extended Data Fig. 1), but median thermal sensitivity is higher for aquatic ectotherms implying that both aquatic and terrestrial ecosystems will experience substantial increases in heat failure rate (median percentage increase, 180% and 774%, respectively, under the SSP2–4.5 scenario<sup>6</sup>; Fig. 3a). Furthermore, the more homogenous thermal conditions in aquatic habitats leave considerably fewer options for behavioural mitigation to avoid stressful temperature exposure<sup>31</sup>. These increases in heat failure rate are much more substantial than the projected 6% and 32% increases in permissive biological rates estimated for aquatic and terrestrial ectotherms, respectively, in association with increases in mean temperature (Fig. 3a and Extended Data Fig. 2).

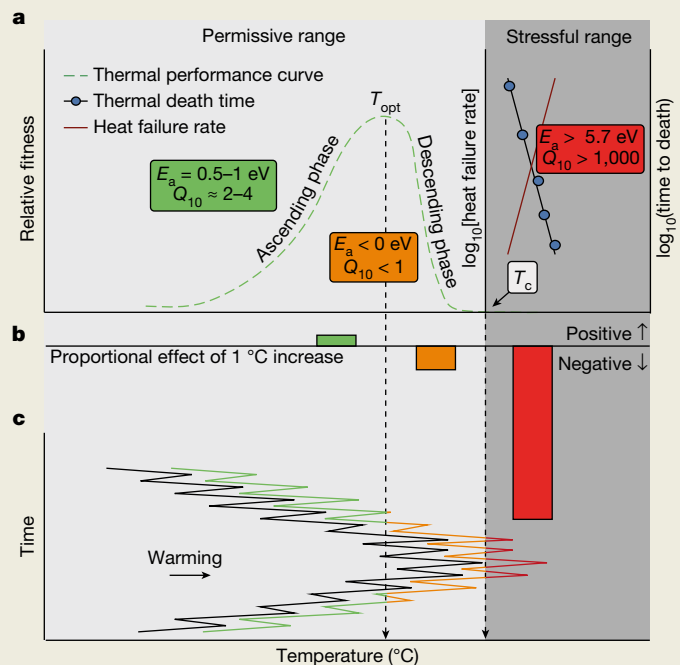
## Box 1

## The impact of global warming on biological rates of life and death

Increases in environmental temperature represent a substantial challenge for ectothermic animals in the Anthropocene<sup>6,36</sup> and there is an urgent need to understand how elevated temperature affects their fitness and survival<sup>3,11,30,37–40</sup>. A stylized road map to assess this problem is shown in the figure with an idealized thermal performance curve for population growth in the permissive temperature range (green curve in **a**) and a thermal death time curve in the stressful temperature range (blue curve in **a**). When global warming increases temperature in the lower permissive range, below the optimal temperature ( $T_{opt}$ ), it increases performance and population growth as discussed for both agricultural and natural ecosystems<sup>15,16,40</sup> (ascending phase in the figure;  $Q_{10}$  for positive fitness, ~2–4). However, population growth rate is progressively reduced when temperature exceeds  $T_{opt}$  along the descending part of the thermal performance curve (descending phase in the figure;  $Q_{10}$  for positive fitness <1). Although population growth persists in this part of the permissive temperature range, the decline in performance is typically more sensitive to temperature change than on the ascending part of the thermal performance curve<sup>11,32,41,42</sup>. The negative effects of increased exposure to permissive temperatures beyond  $T_{opt}$  for population growth have been suggested to challenge particularly tropical species<sup>40,43</sup>.

Exposure to stressful temperatures beyond  $T_c$  is associated with negative fitness (mortality) and inclusion of such extreme temperature exposures instead suggests that mid-latitude species are at risk<sup>5,30,44</sup>. As shown in this study, exposure to increased temperature in the stressful range is associated with a substantial acceleration of heat mortality as temperature effects on survival are characterized by an extreme thermal sensitivity in the stressful range (red curve in **a**, note the logarithmic axis for heat failure rate;  $Q_{10}$  for heat failure rate, >1,000). Accordingly, small increases in maximal temperature exposure can have severe consequences. Together, this schematic illustrates how different temperature ranges have positive or negative effects on performance or survival, but it also shows that these effects have very different temperature sensitivities (summarized in **b**).

To integrate the positive and negative temperature effects of global warming, we argue that models should consider how global warming alters the duration and intensity of exposures within both the permissive and stressful temperature ranges<sup>25,45–47</sup>. Such an approach is shown in **c**, where warming across daily and seasonal temperature variations changes the dynamics of positive and negative temperature effects. The pursuit of these integrative models is complicated by many factors—including acclimatization, behaviour, local adaptation and life stage—but, even so, it will be pivotal to consider the proportional exposure duration in these different temperature ranges. It is therefore critical to establish general methods to determine the  $T_c$ , which is central for risk assessment<sup>22</sup>, but also to understand how the availability of suitable microhabitats and use of behavioural thermoregulation affects operative temperature, which ultimately determines the effect of temperature and climate warming on ectotherms<sup>33,35,48</sup>.



To demonstrate that the risk of exposure to temperatures above  $T_c$  in current and future climate varies within the species distribution, Fig. 3b presents an analysis of two species (*Girella nigricans* and *Pheidole megacephala*). These species-level examples were generated by contrasting current and future (SSP2–4.5 scenario) estimates of maximal environmental temperature against a conservative approximation of  $T_c$  (here calculated as the temperature that causes heat failure in 24 h). Although some populations already experience temperatures above  $T_c$  in their current distribution, climate warming will result in more populations experiencing temperatures exceeding  $T_c$  (Fig. 3b and Extended Data Fig. 3). As evident from Fig. 3c, the consequences of future warming will depend on the current climate and the projected warming but, for some populations, projected warming will exacerbate the heat failure rate relative to current conditions by up to 2,100% and 690% for *G. nigricans* and *P. megacephala*, respectively (Fig. 3c). To put this into context, a 1,000% (tenfold) increase in heat failure rate entails that an ectotherm accumulating 15% of its lethal

thermal injury on a very hot day under current climate conditions, will instead experience 150% of its lethal dose over the same duration under the future warming scenario. As a corollary, a 1,000% increase in failure rate implies that an ectotherm currently surviving for 5 h during a hot day will instead succumb to heat death within 30 min under the future warming scenario.

The general risk analysis for ectotherms in Fig. 3a suggests that both terrestrial and aquatic species may experience substantial increases in the intensity of injurious heat stress. Although terrestrial ectotherms can often escape short-term heat exposures by seeking permissive microhabitats (< $T_c$ )<sup>31–35</sup>, warming may reduce the availability of such microhabitats. In both terrestrial and aquatic environments, there is considerable spatial variation in regional climate warming with projected increases in maximum temperature greater than 8 °C in some regions even in the SSP2–4.5 scenario<sup>6</sup> (Extended Data Fig. 1). As a consequence, the potential increase in heat failure rate for species living close to their  $T_c$  can be even more extreme locally, particularly across

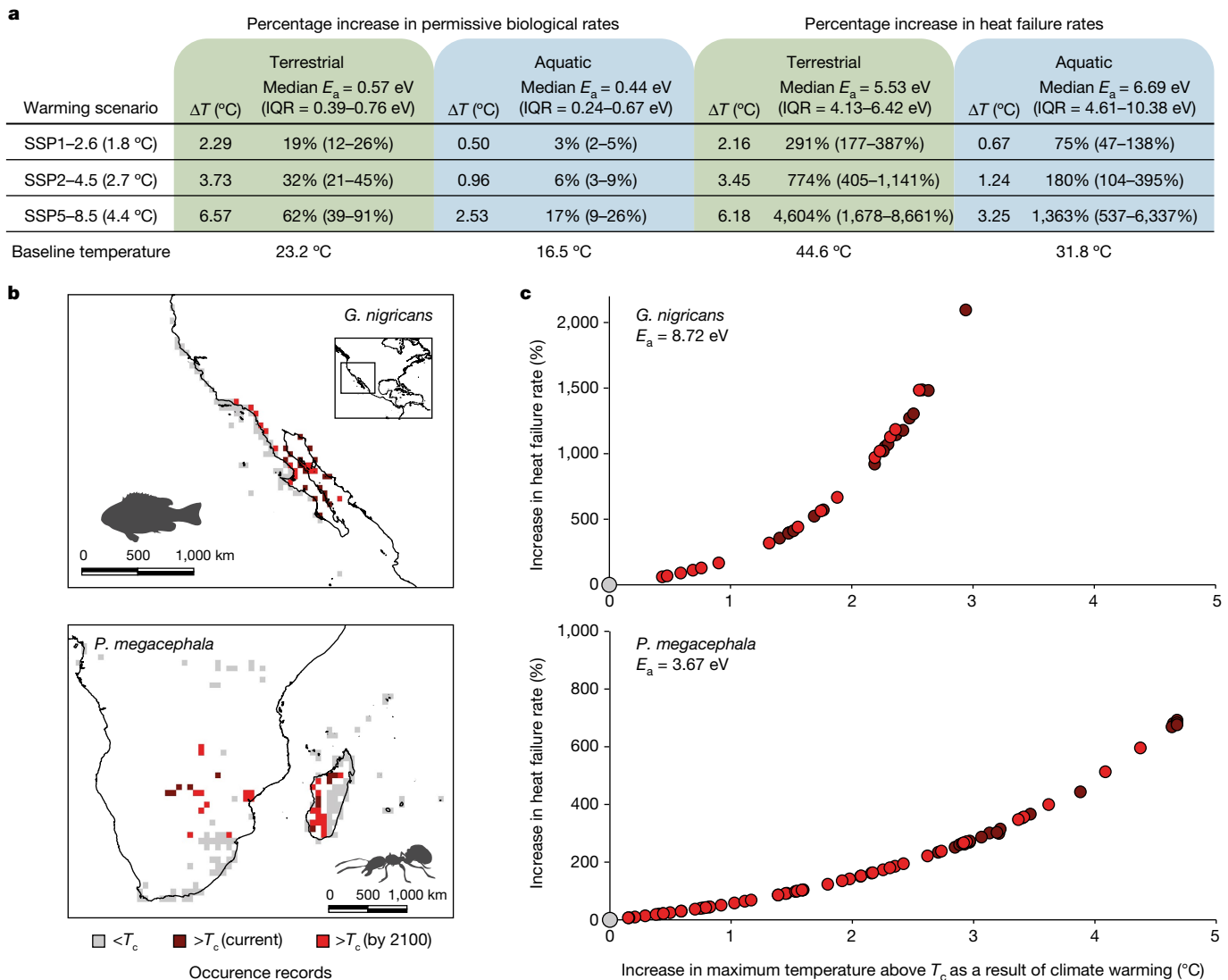


**Fig. 3 | Projected increase in heat failure rate with climate warming.**

**a**, Percentage increases in biological rates associated with future climate change in terrestrial and aquatic environments (in 2081–2100 and 2090–2100, respectively). The temperature change  $\Delta T$  for three warming scenarios<sup>6</sup> corresponds to changes in the mean and maximum temperature for the permissive and stressful range, respectively. SSP1-2.6 is within the limits of the Paris Agreement, whereas SSP2-4.5 and SSP5-8.5 represent intermediate and severe emission scenarios, respectively. Percentage increases in rates (median and IQR) are based on the baseline temperature,  $\Delta T$  and environment-specific  $E_a$  for the permissive and stressful temperature range (Methods; see Extended Data Figs. 2 and 4 for global maps). **b**, Analysis evaluating the risk of exposure to temperatures above the critical temperature  $T_c$  (estimated as the temperature resulting in heat failure in 24 h) for two example species, *G. nigricans* and

*P. megacephala*, in current and future (SSP2–4.5) climates. Occurrence locations are coloured according to the comparison between  $T_c$  and maximal environmental temperature ( $T_{env,max}$ ). Grey,  $T_c > T_{env,max}$  in both current and future climates; maroon,  $T_c < T_{env,max}$  in the current climate; red,  $T_c < T_{env,max}$  in future climates. The global distribution of *P. megacephala* is shown in Extended Data Fig. 3. **c**, Increases in heat failure rate resulting from SSP2–4.5-projected increase in maximal temperature above  $T_c$  using global occurrences and thermal sensitivities for *G. nigricans* and *P. megacephala* (Methods). Colours are as described in **b**. For occurrences in red, the increase in maximal temperature is the difference between future maximum temperature and  $T_c$ . For occurrences in maroon (which already experiences temperatures of  $>T_c$ ), the additional increase in temperature between current and future maximum temperature was used.

temperate terrestrial environments in the Northern Hemisphere and in aquatic environments across the Arctic (Extended Data Figs. 4 and 5).

Using air and sea surface maximum temperatures may further underestimate the exposure to stressful temperature as it does not account for temperatures experienced in particular warm microclimates, nor does it consider that solar radiation and convective heat transfer<sup>3,31,33</sup> can increase the operative temperature considerably above air temperature. By contrast, the risk estimate presented here does not directly account for mitigation through behavioural selection of permissive microhabitats<sup>32–35</sup> or for acclimation/adaptive responses that could alter thermal tolerance<sup>2,7</sup>. Species-specific implications of future heatwaves should therefore consider the local risk of exposure

to extreme events beyond  $T_c$  (Fig. 3b). Nevertheless, most ecosystems will probably include species that are at risk of exposure to temperatures beyond  $T_c$  (ref.<sup>3</sup>).

The risk analysis presented here is mainly relevant for species that experience temperatures above  $T_c$  in their current or future environment (Fig. 3b), and the notable implications primarily pertain to the periods during which environmental temperature is highest. The effect of global warming on processes of life and death should therefore ideally integrate positive and negative warming effects within both the permissive and stressful temperatures (Box 1). Even so, our analysis highlights that heat stress is likely to escalate substantially with even a modest degree of global warming (Fig. 3). The effects of warming on

heat failure rates are several magnitudes greater than the temperature effects previously considered when analysing warming of permissive biological processes. As a consequence, both aquatic and terrestrial ectotherms risk considerable increases in heat stress with global warming and this increase will be accentuated markedly on the regional scale and with each degree of further global warming.

## Online content

Any methods, additional references, Nature Research reporting summaries, source data, extended data, supplementary information, acknowledgements, peer review information; details of author contributions and competing interests; and statements of data and code availability are available at <https://doi.org/10.1038/s41586-022-05334-4>.

1. Angilletta, M. J. *Thermal Adaptation: A Theoretical and Empirical Synthesis* (Oxford Univ. Press, 2009).
2. Cossins, A. R. & Bowler, K. *Temperature Biology of Animals* (Chapman and Hall, 1987).
3. Sunday, J. M. et al. Thermal-safety margins and the necessity of thermoregulatory behavior across latitude and elevation. *Proc. Natl Acad. Sci. USA* **111**, 5610–5615 (2014).
4. Perry, A. L., Low, P. J., Ellis, J. R. & Reynolds, J. D. Climate change and distribution shifts in marine fishes. *Science* **308**, 1912–1915 (2005).
5. Kellermann, V. et al. Upper thermal limits of *Drosophila* are linked to species distributions and strongly constrained phylogenetically. *Proc. Natl Acad. Sci. USA* **109**, 16228–16233 (2012).
6. IPCC. *Climate Change 2021: The Physical Science Basis* (eds Masson-Delmotte, V. et al.) (Cambridge Univ. Press, 2021).
7. Hofmann, G. E. & Todgham, A. E. Living in the now: physiological mechanisms to tolerate a rapidly changing environment. *Annu. Rev. Physiol.* **72**, 127–145 (2010).
8. Schulte, P. M. The effects of temperature on aerobic metabolism: towards a mechanistic understanding of the responses of ectotherms to a changing environment. *J. Exp. Biol.* **218**, 1856–1866 (2015).
9. Sunday, J. et al. Thermal tolerance patterns across latitude and elevation. *Philos. Trans. R. Soc. B* **374**, 20190036 (2019).
10. Parratt, S. R. et al. Temperatures that sterilize males better match global species distributions than lethal temperatures. *Nat. Clim. Change* **11**, 481–484 (2021).
11. Sunday, J. M., Bates, A. E. & Dulvy, N. K. Thermal tolerance and the global redistribution of animals. *Nat. Clim. Change* **2**, 686–690 (2012).
12. Schmidt-Nielsen, K. *Animal physiology: Adaptation and Environment* 5th edn (Cambridge Univ. Press, 1997).
13. Dell, A. I., Pawar, S. & Savage, V. M. Systematic variation in the temperature dependence of physiological and ecological traits. *Proc. Natl Acad. Sci. USA* **108**, 10591–10596 (2011).
14. Seebacher, F., White, C. R. & Franklin, C. E. Physiological plasticity increases resilience of ectothermic animals to climate change. *Nat. Clim. Change* **5**, 61–66 (2014).
15. Dillon, M. E., Wang, G. & Huey, R. B. Global metabolic impacts of recent climate warming. *Nature* **467**, 704–706 (2010).
16. Deutsch, C. A. et al. Increase in crop losses to insect pests in a warming climate. *Science* **361**, 916–919 (2018).
17. Jørgensen, L. B., Malte, H. & Overgaard, J. How to assess *Drosophila* heat tolerance: unifying static and dynamic tolerance assays to predict heat distribution limits. *Funct. Ecol.* **33**, 629–642 (2019).
18. Hollingsworth, M. J. Temperature and length of life in *Drosophila*. *Exp. Gerontol.* **4**, 49–55 (1969).
19. Fry, F. E. J., Hart, J. S. & Walker, K. F. *Lethal Temperature Relations for a Sample of Young Speckled Trout*, *Salvelinus fontinalis* 9–35 (Univ. Toronto, 1946).
20. MacLean, H. J. et al. Evolution and plasticity of thermal performance: an analysis of variation in thermal tolerance and fitness in 22 *Drosophila* species. *Philos. Trans. R. Soc. B* **374**, 20180548 (2019).
21. Pörtner, H.-O. & Farrell, A. P. Physiology and climate change. *Science* **322**, 690–692 (2008).
22. Ørsted, M., Jørgensen, L. B. & Overgaard, J. Finding the right thermal limit: a framework to reconcile ecological, physiological, and methodological aspects of  $CT_{max}$  in ectotherms. *J. Exp. Biol.* **225**, jeb244514 (2022).
23. Brown, J. H., Gillooly, J. F., Alle, A. P., Savage, V. M. & West, G. B. Toward a metabolic theory of ecology. *Ecology* **85**, 1771–1789 (2004).
24. Munch, S. B. & Salinas, S. Latitudinal variation in lifespan within species is explained by the metabolic theory of ecology. *Proc. Natl Acad. Sci. USA* **106**, 13860–13864 (2009).
25. Jørgensen, L. B., Malte, H., Ørsted, M., Klahn, N. A. & Overgaard, J. A unifying model to estimate thermal tolerance limits in ectotherms across static, dynamic and fluctuating exposures to thermal stress. *Sci. Rep.* **11**, 12840 (2021).
26. Rezende, E. L., Castañeda, L. E. & Santos, M. Tolerance landscapes in thermal ecology. *Funct. Ecol.* **28**, 799–809 (2014).
27. Bowler, K. Heat death in poikilotherms: is there a common cause? *J. Therm. Biol.* **76**, 77–79 (2018).
28. Somero, G. N. The physiology of climate change: how potentials for acclimatization and genetic adaptation will determine ‘winners’ and ‘losers’. *J. Exp. Biol.* **213**, 912–920 (2010).
29. Buckley, L. B., Huey, R. B. & Kingsolver, J. G. Asymmetry of thermal sensitivity and the thermal risk of climate change. *Glob. Ecol. Biogeogr.* **31**, 2231–2244 (2022).
30. Overgaard, J., Kearney, M. R. & Hoffmann, A. A. Sensitivity to thermal extremes in Australian *Drosophila* implies similar impacts of climate change on the distribution of widespread and tropical species. *Glob. Change Biol.* **20**, 1738–1750 (2014).
31. Pinsky, M. L., Eikeset, A. M., McCauley, D. J., Payne, J. L. & Sunday, J. M. Greater vulnerability to warming of marine versus terrestrial ectotherms. *Nature* **569**, 108–111 (2019).
32. Huey, R. B. et al. Predicting organismal vulnerability to climate warming: roles of behaviour, physiology and adaptation. *Philos. Trans. R. Soc. B* **367**, 1665–1679 (2012).
33. Kearney, M., Shine, R. & Porter, W. P. The potential for behavioral thermoregulation to buffer cold-blooded’ animals against climate warming. *Proc. Natl Acad. Sci. USA* **106**, 3835–3840 (2009).
34. Woods, H. A., Dillon, M. E. & Pincebourde, S. The roles of microclimatic diversity and of behavior in mediating the responses of ectotherms to climate change. *J. Therm. Biol.* **54**, 86–97 (2015).
35. Stevenson, R. D. The relative importance of behavioral and physiological adjustments controlling body temperature in terrestrial ectotherms. *Am. Nat.* **126**, 362–386 (1985).
36. Chen, I., Hill, J. K., Ohlemüller, R., Roy, D. B. & Thomas, C. D. Rapid range shifts of species associated with high levels of climate warming. *Science* **333**, 1024–1026 (2011).
37. Buckley, L. B. & Kingsolver, J. G. Functional and phylogenetic approaches to forecasting species’ responses to climate change. *Annu. Rev. Ecol. Evol. Syst.* **43**, 205–226 (2012).
38. Roeder, K. A., Bujan, J., de Beurs, K. M., Weiser, M. D. & Kaspari, M. Thermal traits predict the winners and losers under climate change: an example from North American ant communities. *Ecosphere* **12**, e03645 (2021).
39. Penick, C. A., Diamond, S. E., Sanders, N. J. & Dunn, R. R. Beyond thermal limits: comprehensive metrics of performance identify key axes of thermal adaptation in ants. *Funct. Ecol.* **31**, 1091–1100 (2017).
40. Deutsch, C. A. et al. Impacts of climate warming on terrestrial ectotherms across latitude. *Proc. Natl Acad. Sci. USA* **105**, 6668–6672 (2008).
41. Huey, R. B. & Stevenson, R. D. Integrating thermal physiology and ecology of ectotherms: a discussion of approaches. *Integr. Comp. Biol.* **19**, 357–366 (1979).
42. Sinclair, B. J. et al. Can we predict ectotherm responses to climate change using thermal performance curves and body temperatures? *Ecol. Lett.* **19**, 1372–1385 (2016).
43. Tewksbury, J. J., Huey, R. B. & Deutsch, C. A. Putting the heat on tropical animals the scale of prediction. *Science* **320**, 1296–1297 (2008).
44. Kingsolver, J. G., Diamond, S. E. & Buckley, L. B. Heat stress and the fitness consequences of climate change for terrestrial ectotherms. *Funct. Ecol.* **27**, 1415–1423 (2013).
45. Kingsolver, J. G. & Woods, H. A. Beyond thermal performance curves: modeling time-dependent effects of thermal stress on ectotherm growth rates. *Am. Nat.* **187**, 283–294 (2016).
46. Kingsolver, J. G., Higgins, J. K. & Augustine, K. E. Fluctuating temperatures and ectotherm growth: distinguishing non-linear and time-dependent effects. *J. Exp. Biol.* **218**, 2218–2225 (2015).
47. Clusella-Trullas, S., Garcia, R. A., Terblanche, J. S. & Hoffmann, A. A. How useful are thermal vulnerability indices? *Trends Ecol. Evol.* **36**, 1000–1010 (2021).
48. Pincebourde, S. & Casas, J. Narrow safety margin in the phyllosphere during thermal extremes. *Proc. Natl Acad. Sci. USA* **116**, 5588–5596 (2019).

**Publisher’s note** Springer Nature remains neutral with regard to jurisdictional claims in published maps and institutional affiliations.

Springer Nature or its licensor holds exclusive rights to this article under a publishing agreement with the author(s) or other rightsholder(s); author self-archiving of the accepted manuscript version of this article is solely governed by the terms of such publishing agreement and applicable law.

© The Author(s), under exclusive licence to Springer Nature Limited 2022

## Methods

### Data collection for the meta-analysis

To estimate the thermal sensitivity of permissive biological rates, we collected data for a meta-analysis of processes covering enzyme activity, heart rate, locomotion, feeding and metabolic rate for a wide range of ectothermic animal species. The dataset includes 1,351 entries of biological rates measured at two temperatures and represents 314 species examined in 304 original publications. Data were mostly sourced from two large collections of published data compiled by Dell et al. (see Supporting Information in ref.<sup>13</sup>) (here we used only  $E_a$  of the ascending rates derived from trait performance curves) and by Seebacher et al. (see Supplementary Information in ref.<sup>14</sup>), and overlapping entries were removed. A few ( $n = 4$ ) additional entries were included as they were used as examples in Fig. 2a.

To estimate the thermal sensitivity of heat failure rates in the highly stressful temperature range, we compiled data on time to heat failure with associated test temperatures. This dataset includes 123 thermal sensitivities for 112 species. Data were compiled from 69 individual studies and an additional 54 studies sourced from references reported by Rezende et al. (see Supporting Information in ref.<sup>26</sup>), and were included only if heat failure times were available for at least three temperatures.

### Calculation of $E_a$

The Arrhenius activation energy  $E_a$  was calculated to quantify the thermal sensitivity of rates related to either permissive or stressful biological processes. The  $E_a$  values of ascending rates (in the permissive temperature range) originating from Supporting Information in ref.<sup>13</sup> were available from the publication, whereas  $E_a$  values for all other rates were calculated using a linear regression in an Arrhenius analysis. **The Arrhenius analysis was performed by regressing the natural logarithm to the rate against the reciprocal temperature (1/temperature (K<sup>-1</sup>)).** The regression slope was then used to calculate the activation energy  $E_a$

$$E_a = \frac{-R \times \text{slope}}{N_A \times C} \quad (1)$$

Where  $R$  is the gas constant (8.31 J K<sup>-1</sup> mol<sup>-1</sup>),  $N_A$  is the Avogadro constant ( $6.022 \times 10^{23}$  mol<sup>-1</sup>), and  $C$  is a conversion factor to report  $E_a$  in eV ( $1.602 \times 10^{-19}$  J eV<sup>-1</sup>).

To estimate activation energy  $E_a$  for heat failure rates in the stressful temperature range, we calculated heat failure rates (min<sup>-1</sup>) by converting the collected heat failure times (min) as

$$\text{Heat failure rate} = 1/\text{heat failure time} \quad (2)$$

Accordingly, heat failure rate represents the incremental heat stress that accumulates per minute at a specific constant temperature and, once the increments sum to 1, heat failure occurs (that is, the number of increments (time) to sum to 1 equals the heat failure time). For example, if heat failure time is 100 min at 38 °C, then the corresponding heat failure rate at 38 °C is  $1/100 \text{ min} = 0.01 \text{ min}^{-1}$  and, therefore, accumulating these increments of heat stress over a 100 min exposure to 38 °C results in summation to 1 = heat failure.

The median heat failure times used to calculate  $E_a$  vary between studies (median = 125 min, IQR = 31.5–422 min) but a linear regression of  $\log_{10}[\text{median duration}]$  against  $E_a$  did not reveal any significant correlation ( $F_{1,121} = 0.36$ ,  $P = 0.55$ ,  $R^2 < 0.01$ ), and we therefore conclude that high  $E_a$  is not an artefact of test duration.

### Converting $E_a$ to estimates of $Q_{10}$

In mainstream literature, thermal sensitivities are often presented using the thermal sensitivity quotient  $Q_{10}$  (that is, the factorial change in rate associated with a 10 °C temperature change). To discuss thermal

sensitivities using the more commonplace  $Q_{10}$ , we converted activation energy  $E_a$  using

$$Q_{10} = e^{\frac{10K \times E_a}{k_B \times T^2}} \quad (3)$$

Where  $E_a$  is the activation energy (eV),  $k_B$  is the Boltzmann constant ( $8.617 \times 10^{-5}$  eV K<sup>-1</sup>) and  $T$  is the temperature (K). This conversion is sensitive to temperature and here we used the temperature  $T = 18.3$  °C (291.5 K) for conversion to permissive  $Q_{10}$  and  $T = 36.3$  °C (309.5 K) for stressful  $Q_{10}$ . These temperatures were chosen as they represent the mean temperature used to measure the rates in the permissive and stressful temperature range, respectively.

### Modelling projected temperature change

To model the impact of increased intensity of heatwaves, we associated the predicted rise in future temperature with the thermal sensitivity  $E_a$  in terrestrial and aquatic environments. To make this change spatially and temporally explicit, we used projected global changes in mean and maximum temperature for three different emission scenarios (see below) towards the end of the twenty-first century compared with present-day conditions (Extended Data Fig. 1).

For terrestrial areas, we used the WorldClim v.2.1 climate database (<https://worldclim.org>)<sup>49</sup>, based on monthly averages, using the bioclimatic variables ‘mean annual temperature’ (BIO1) and ‘maximum temperature of the warmest month’ (BIOS). In WorldClim, present conditions are produced with monthly averages for the latest climate period 1970–2000. Future layers of mean and maximum temperature (BIO1 and BIOS, respectively) were produced by averaging data from eight general circulation models (GCMs) (Extended Data Table 2) for the period 2081–2100. We used projected changes for three future Shared Socioeconomic Pathways (SSP) scenarios<sup>6</sup>: (1) the optimistic SSP1–2.6, a peak-and-decline scenario ending with low greenhouse gas concentration levels by the end of the twenty-first century; (2) the SSP2–4.5 ‘middle of the road’ scenario where trends do not shift markedly from historical patterns; and (3) the pessimistic and perhaps unrealistic SSP5–8.5, where fossil-fuelled development increases emissions over time leading to high greenhouse gas concentrations (for discussions on the use and misuse of emission scenarios, see refs.<sup>50–52</sup>).

For aquatic areas, we used the Bio-ORACLE v.2.0 database (<https://bio-oracle.org/>)<sup>53,54</sup>, based on monthly averages, using the variables average and maximum sea surface water temperature (SST). In Bio-ORACLE, present conditions are produced with monthly averages for the period 2000–2014. Future layers of mean and maximum SST were produced by averaging data from three atmosphere–ocean coupled GCMs (AO-GCMs) (Extended Data Table 2) for the period 2090–2100. The SSPs are not yet available for aquatic environments, so we used the corresponding Representative Concentration Pathway (RCP) scenarios (RCP2.6, RCP4.5, and RCP8.5, respectively) that precede the SSP scenarios (hereafter, we refer to all scenarios by the corresponding SSP). In terms of temperature change by the end of the twenty-first century, the SSPs and RCPs yield practically identical predictions<sup>52</sup>. All spatial data were used at a 5 arcmin resolution in a Behrmann equal area cylindrical projection (approximately 9.2 km) with the WGS84 datum.

### Exposure to temperatures above $T_c$

In two example species (*G. nigricans* and *P. megacephala*), we estimated exposure to environmental temperatures above the critical temperature  $T_c$  separating the permissive and stressful temperature range. In this analysis we first established a proxy of  $T_c$  representing the temperature above which heat stress accumulates. Specifically,  $T_c$  (K) is estimated as the temperature causing heat failure after 24 h, using the slope and intercept from the linear regression in the Arrhenius analysis

$$T_c = \frac{\text{slope}}{\ln(R') - \text{intercept}} \quad (4)$$

Where  $R'$  is the rate calculated to result in heat failure after 24 h (that is,  $R' = 1/1,440$  min, compare with equation (2)). This approximation of  $T_c$  is conservative as the linearity of heat failure rates often extends beyond 24 h (for example, Fig. 1a), suggesting that we may underestimate the risk of exposure to temperatures above  $T_c$ . However, the potent nature of heat failure versus temperature discourages excessive extrapolation of such data (see the discussions in refs. <sup>17,25</sup>).

For the species-level risk assessment, we then obtained occurrence records from the Global Biodiversity Information Facility (GBIF; <https://www.gbif.org/>; downloaded 20 March 2022). After removal of faulty records, we found 647 and 2,063 occurrences for *G. nigricans* and *P. megacephala*, respectively, from which we extracted the maximum temperature in the current climate and from the SSP2–4.5 future warming scenario (BIO5 (terrestrial) and maximum SST (aquatic) for *P. megacephala* and *G. nigricans*, respectively). Temperature data were aggregated within  $46 \times 46$  km and  $92 \times 92$  km cells for *G. nigricans* and *P. megacephala*, respectively, to avoid sampling bias, resulting in 93 and 403 cells for *G. nigricans* and *P. megacephala*, respectively. The maximum environmental temperatures at these locations were evaluated against the species-specific estimates of  $T_c$  to determine which of the occurrence locations experience temperatures  $\geq T_c$  now and under future warming. The increase in maximal environmental temperature above  $T_c$  was associated with the resulting increase in heat failure rates using species-specific  $E_a$  estimates (8.72 eV and 3.67 eV for *G. nigricans* and *P. megacephala*, respectively), and  $T_c$  (31.5 °C and 34.4 °C for *G. nigricans* and *P. megacephala*, respectively). For the parts of the species-distribution ranges in which populations experience temperatures above  $T_c$  only after future climate warming, the increase in maximal temperature was calculated as the difference between the future maximum temperature and  $T_c$ . For the populations in which maximal temperature already exceeds  $T_c$ , the increase in temperature was calculated from the increase between current and projected future maximum temperatures.

### Associating temperature change with $E_a$

The projections on future percentage increases in biological rates in the permissive temperature range were based on the mean annual temperature, whereas projections for increases in heat failure rates were based on the maximum temperatures (Extended Data Fig. 1a,b, respectively). The projected change in local temperature ( $\Delta T$ ) for the three future scenarios (SSP1–2.6, SSP2–4.5 and SSP5–8.5) was determined as follows:

$$\Delta T = T_{\text{future}} - T_{\text{present}} \quad (5)$$

Where  $T_{\text{future}}$  is the mean annual or maximum temperature for the specific future climate scenario, and  $T_{\text{present}}$  is the current mean annual or maximum temperature, and both were calculated separately for the terrestrial and aquatic environment. The current mean annual temperature was described by BIO1 or  $SST_{\text{mean}}$  for terrestrial and aquatic environments, respectively, and the current maximum temperature was described by BIO5 or  $SST_{\text{max}}$  for terrestrial and aquatic environments, respectively (see the ‘Modelling projected temperature change’ section; Extended Data Fig. 1c–h).

Subsequently, the projected change in temperature  $\Delta T$  (mean and maximum for terrestrial and aquatic environments separately) was associated with the activation energy  $E_a$  (median and first–third quartile) for the specific group to calculate the increase in rate, for example,  $E_a$  for heat failure rate in terrestrial ectotherms was associated with  $\Delta T$  based on the maximum temperature in the terrestrial environment. The projected percentage increase in rates (in the permissive and stressful range) was calculated as follows:

$$\Delta \text{Rate} (\%) = \left( \frac{E_a \times \frac{\Delta T}{T_2 - T_1}}{e k_B} - 1 \right) \times 100\% \quad (6)$$

Where  $E_a$  is the activation energy (eV),  $k_B$  is the Boltzmann constant ( $8.617 \times 10^{-5}$  eV K<sup>-1</sup>),  $\Delta T$  is the projected change in temperature (K) between the current and future climate scenario, and  $T_2$  and  $T_1$  are the future and current temperature [K], respectively. The following values of  $E_a$  were used for rates in the permissive temperature range:  $E_a = 0.56839$  eV (terrestrial) and  $E_a = 0.44329$  eV (aquatic); and for heat failure rates:  $E_a = 5.52589$  eV (terrestrial) and  $E_a = 6.68649$  eV (aquatic). These values are also presented in Fig. 3a, and the projected percentage increases in rates resulting from all three future scenarios are shown in Extended Data Fig. 2 (biological rates in the permissive temperature range) and in Extended Data Fig. 4 (heat failure rates in the stressful temperature range).

Equation (6) was also used to calculate the percentage increase in rates from a 1 °C temperature increase, using the median  $E_a$  for the permissive biological rates ( $E_a = 0.48$  eV) or heat failure rates ( $E_a = 6.13$  eV) disregarding the specific environment and using the temperatures listed in the ‘Converting  $E_a$  to estimates of  $Q_{10}$ ’ section.

### Reporting summary

Further information on research design is available in the Nature Research Reporting Summary linked to this article.

### Data availability

The data supporting the findings of this study are available online<sup>55</sup>.

49. Fick, S. E. & Hijmans, R. J. WorldClim 2: new 1-km spatial resolution climate surfaces for global land areas. *Int. J. Climatol.* **37**, 4302–4315 (2017).
50. Moss, R. H. et al. The next generation of scenarios for climate change research and assessment. *Nature* **463**, 747–756 (2010).
51. Hausfather, Z. & Peters, G. P. Emissions—the ‘business as usual’ story is misleading. *Nature* **577**, 618–620 (2020).
52. Tollefson, J. How hot will Earth get by 2100? *Nature* **580**, 443–445 (2020).
53. Assis, J. et al. Bio-ORACLE v2.0: extending marine data layers for bioclimatic modelling. *Glob. Ecol. Biogeogr.* **27**, 277–284 (2018).
54. Tyberghein, L. et al. Bio-ORACLE: a global environmental dataset for marine species distribution modelling. *Glob. Ecol. Biogeogr.* **21**, 272–281 (2012).
55. Jørgensen, L. B., Ørsted, M., Malte, H., Wang, T. & Overgaard, J. Data from: Extreme escalation of heat failure rates in ectotherms with global warming. Zenodo <https://doi.org/10.5281/zenodo.6979789> (2022).
56. Grove, T. J., McFadden, L. A., Chase, P. B. & Moerland, T. S. Effects of temperature, ionic strength and pH on the function of skeletal muscle myosin from a eurythermal fish, *Fundulus heteroclitus*. *J. Muscle Res. Cell Motil.* **26**, 191–197 (2005).
57. Doudoroff, P. The resistance and acclimatization of marine fishes to temperature changes. II. Experiments with *Fundulus* and *Atherinops*. *Biol. Bull.* **88**, 194–206 (1945).
58. Sirikharin, R., Söderhäll, I. & Söderhäll, K. Characterization of a cold-active transglutaminase from a crayfish, *Pacifastacus leniusculus*. *Fish Shellfish Immunol.* **80**, 546–549 (2018).
59. Becker, C. D. & Genoway, R. G. Resistance of crayfish to acute thermal shock: preliminary studies. in *Proc. Thermal Ecology NTIS Conf. 730505* (eds Gibbons, J. W. & Sharitz, R. R.) 146–150 (NTIS, 1974).
60. Widdows, J. Effect of temperature and food on the heart beat, ventilation rate and oxygen uptake of *Mytilus edulis*. *Mar. Biol.* **20**, 269–276 (1973).
61. Wallis, R. L. Thermal tolerance of *Mytilus edulis* of eastern Australia. *Mar. Biol.* **30**, 183–191 (1975).
62. Gray, J. The mechanism of ciliary movement. III. The effect of temperature. *Proc. R. Soc. B* **95**, 6–15 (1923).
63. Shertzer, R. H., Hart, R. G. & Pavlick, F. M. Thermal acclimation in selected tissues of the leopard frog *Rana pipiens*. *Comp. Biochem. Physiol. A* **51**, 327–334 (1975).
64. Orr, P. R. Heat death. II. Differential response of entire animal (*Rana pipiens*) and several organ systems. *Physiol. Zool.* **28**, 294–302 (1955).
65. Lighton, J. R. B. & Duncan, F. D. Energy cost of locomotion: validation of laboratory data by *in situ* respirometry. *Ecology* **83**, 3517–3522 (2002).
66. Heatwole, H. & Harrington, S. Heat tolerances of some ants and beetles from the pre-Saharan steppe of Tunisia. *J. Arid Environ.* **16**, 69–77 (1989).

**Acknowledgements** We thank our colleagues at the Section for Zoophysiology, Aarhus University for the many discussions on temperature biology of animals. This work was funded by The Danish Council for Independent Research—Natural Sciences (to J.O.) and The Danish Council for Independent Research—Technology and Production Sciences (to M.Ø.).

**Author contributions** L.B.J., M.Ø. and J.O. conceptualized the study and all of the authors participated in its design. L.B.J., M.Ø., H.M. and J.O. collected the data and performed the analysis. L.B.J. curated the data. L.B.J., M.Ø., T.W. and J.O. wrote and visualized the original draft, and all of the authors contributed to the review and editing of the final manuscript.

**Competing interests** The authors declare no competing interests.

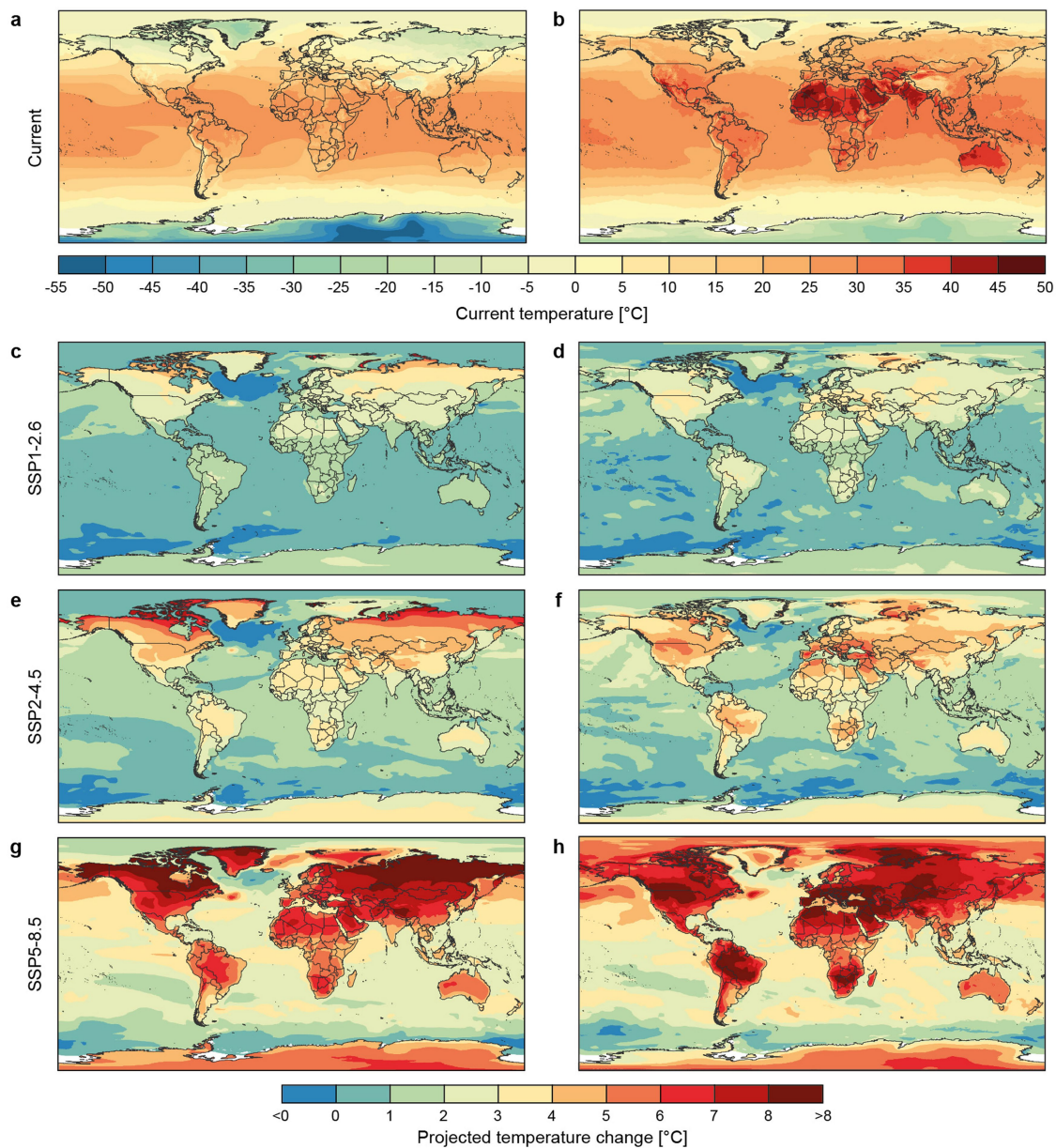
**Additional information**

**Supplementary information** The online version contains supplementary material available at <https://doi.org/10.1038/s41586-022-05334-4>.

**Correspondence and requests for materials** should be addressed to Johannes Overgaard.

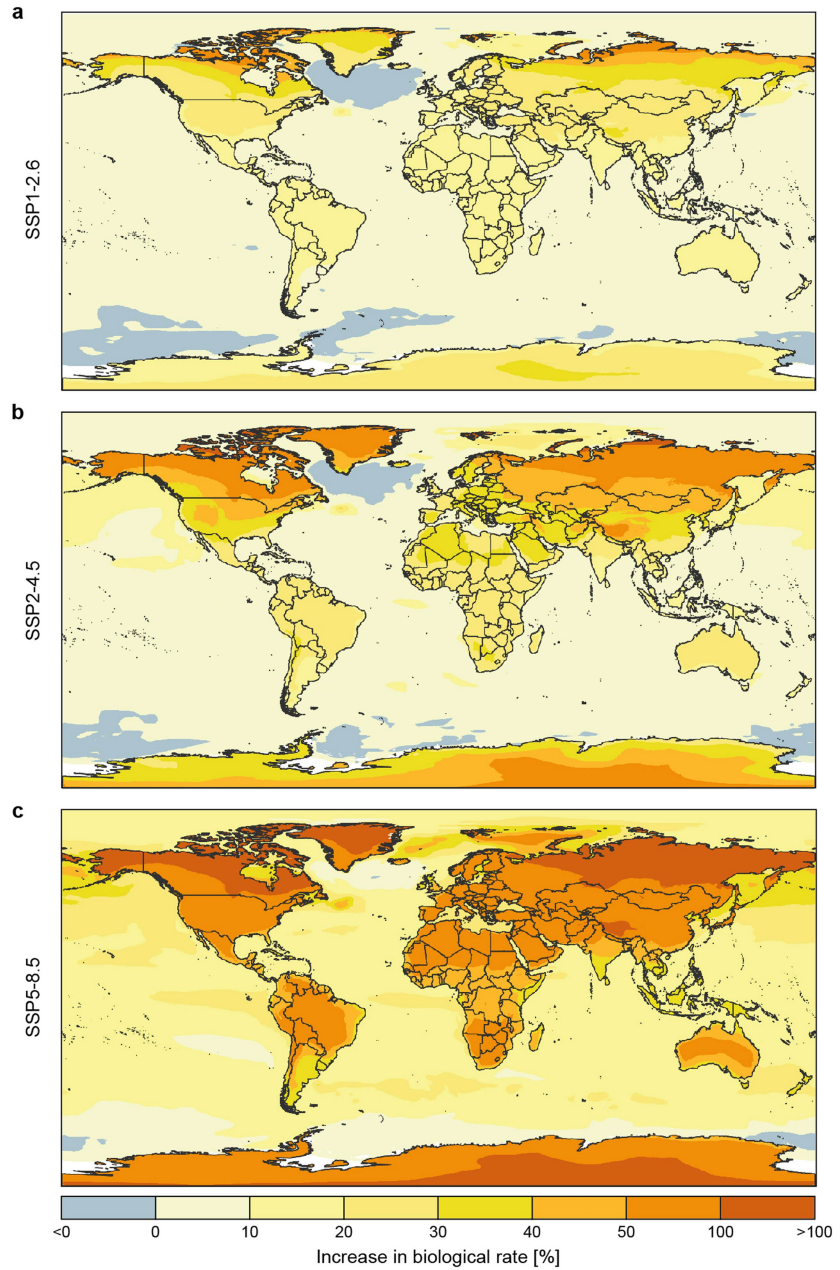
**Peer review information** *Nature* thanks Raymond Huey, David Vasseur and the other, anonymous, reviewer(s) for their contribution to the peer review of this work. Peer reviewer reports are available.

**Reprints and permissions information** is available at <http://www.nature.com/reprints>.



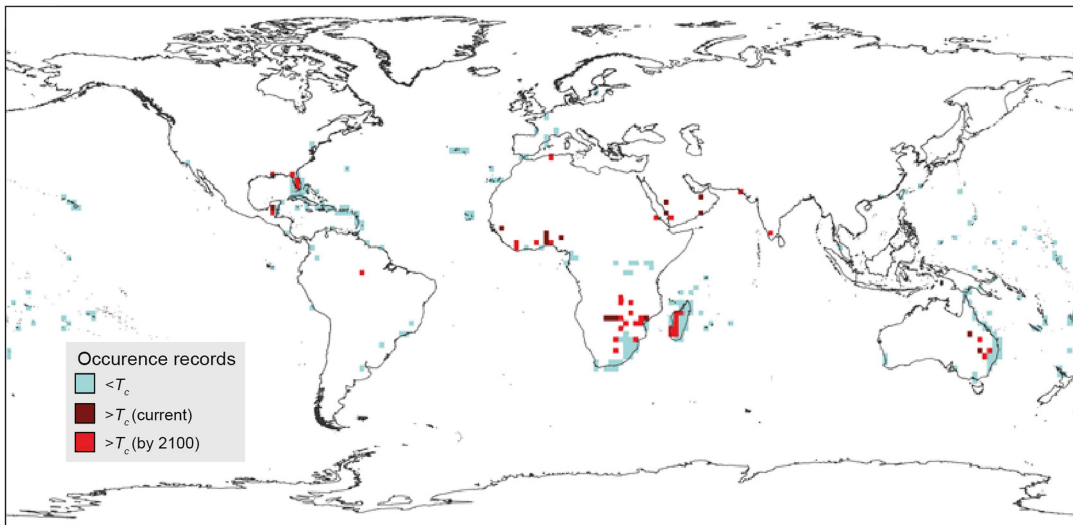
**Extended Data Fig. 1 | Current and projected change in mean and maximum temperature under climate warming.** **a**, Current mean annual temperature described by BIO1 or  $SST_{mean}$  for terrestrial and aquatic environments, respectively. **b**, Current maximum temperature described by BIO5 or  $SST_{max}$  for terrestrial and aquatic environments, respectively. **(a–b)** share the legend immediately below. **c–d**, Projected change in **(c)** mean annual temperature and **(d)** maximum temperature under the SSP1-2.6 scenario. **e–f**, Projected change

in **(e)** mean annual temperature and **(f)** maximum temperature under the SSP2-4.5 scenario. **g–h**, Projected change in **(g)** mean annual temperature and **(h)** maximum temperature under the SSP5-8.5 scenarios. **(c–h)** share the bottom legend and the future period is 2081–2100 for terrestrial environments and 2090–2100 for aquatic environments, as they appear in WorldClim 2.1<sup>49</sup> and Bio-ORACLE 2.0<sup>53,54</sup>, respectively. White areas indicate that temperature data were not available.



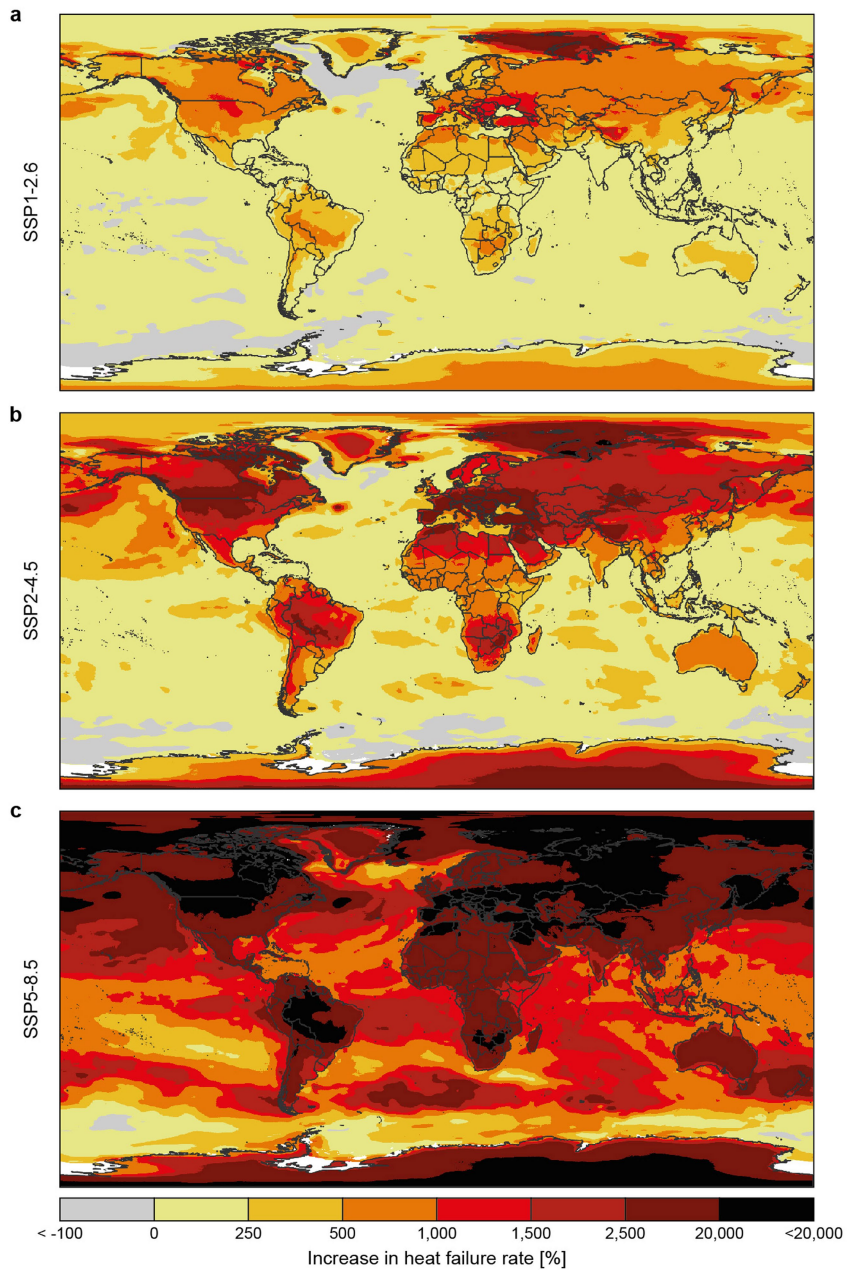
**Extended Data Fig. 2 | Projected increase in biological rates of permissive processes under climate warming.** Increase in biological rates (in %) of permissive processes for both terrestrial ( $E_a = 0.57$  eV) and aquatic species ( $E_a = 0.44$  eV) resulting from changes in annual mean temperature under the (a) SSP1-2.6, (b) SSP2-4.5 and (c) SSP5-8.5 scenario. The future period is 2081-2100

for terrestrial environments and 2090-2100 for aquatic environments, as they appear in WorldClim 2.1<sup>49</sup> and Bio-ORACLE 2.0<sup>53,54</sup>, respectively. White areas indicate that temperature data were not available to calculate the increase in biological rate.



**Extended Data Fig. 3 | Risk of exposure to environmental temperatures above  $T_c$  for *Pheidole megacephala*.** Global risk analysis evaluating exposure to environmental (air) temperatures beyond the critical temperature  $T_c$  (separating the permissive and stressful temperature range, here calculated as the temperature causing heat failure in 24 h) in current and future climates (2081-2100, SSP2-4.5). Occurrence locations in the global distribution of

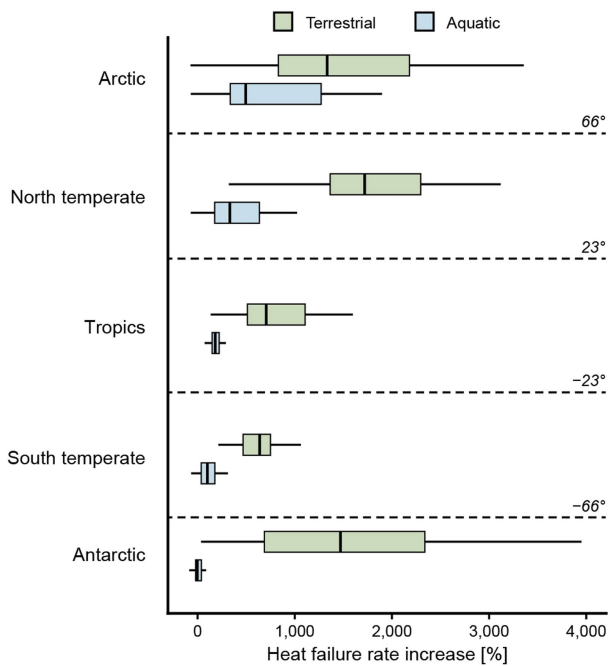
*P. megacephala* are coloured according to the comparison of  $T_c$  to maximal air temperature ( $T_{airmax}$ ). Grey,  $T_c > T_{airmax}$  in current and future climates; red,  $T_c < T_{airmax}$  in the future climate scenarios; maroon,  $T_c < T_{airmax}$  in the current climate. Occurrence records were aggregated to 184 km cells for increased visibility, and a section of the distribution found in Southern Africa is shown in Fig. 3b, with slight discrepancies due to different spatial resolutions of occupied cells.



**Extended Data Fig. 4 | Projected increase in heat failure rates under climate warming.** Increase in heat failure rates (in %) for both terrestrial ( $E_a = 5.53$  eV) and aquatic species ( $E_a = 6.69$  eV) resulting from changes in maximum temperature under the (a) SSP1-2.6, (b) SSP2-4.5 and (c) SSP5-8.5 scenario. The

future period is 2081-2100 for terrestrial environments and 2090-2100 for aquatic environments, as they appear in WorldClim 2.1<sup>49</sup> and Bio-ORACLE 2.0<sup>53,54</sup>, respectively. White areas indicate that temperature data were not available to calculate the heat failure rate increase.

# Article



## Extended Data Fig. 5 | Summary of increases in heat failure rate across latitudes.

**latitudes.** Boxplots of terrestrial and aquatic heat failure rates under the SSP2-4.5 warming scenario across five latitudinal clines summarizing the results reported in Extended Data Fig. 4b. The boxplot midline represents the median, the lower and upper line of the box represents the 1<sup>st</sup> and 3<sup>rd</sup> quartile, respectively (with whiskers extending up to 1.5 times this range), outliers not shown.

**Extended Data Table 1 | Overview of the species used for the representative rates in Fig. 2a,c**

Group	Biological process [unit]	Species <sup>reference</sup>	
		Permissive biological rate	Heat failure rate
Fishes	ATPase Actin activated Mg-ATPase [P <sub>i</sub> s <sup>-1</sup> myosin <sup>-1</sup> ]	<i>Fundulus heteroclitus</i> <sup>56</sup>	<i>Fundulus parvipinnis</i> <sup>57</sup>
Crustaceans	Enzyme Transglutaminase activity [ΔOD <sub>450</sub> s <sup>-1</sup> ]	<i>Pacifastacus leniusculus</i> <sup>58</sup>	<i>Pacifastacus leniusculus</i> <sup>59</sup>
Molluscs	Cardiac Heart rate [beats s <sup>-1</sup> ]	<i>Mytilus edulis</i> <sup>60</sup>	<i>Mytilus edulis</i> <sup>61</sup>
	Feeding Ciliary movement [cm min <sup>-1</sup> ]	<i>Mytilus edulis</i> <sup>62</sup>	
Amphibians	Metabolic rate Muscle O <sub>2</sub> consumption rate [μL O <sub>2</sub> mg <sup>-1</sup> h <sup>-1</sup> ]	<i>Rana pipiens</i> <sup>63</sup>	<i>Rana pipiens</i> <sup>64</sup>
Insects	Locomotion Running speed [m s <sup>-1</sup> ]	<i>Messor pergandei</i> <sup>65</sup>	<i>Messor collingwoodi</i> <sup>66</sup>

Overview of the species used to represent the biological processes and their [units] in the permissive temperature range and the heat failure rates in the stressful temperature range. Species were chosen based on the availability of heat failure rates and matched with measurements of permissive biological rates preferably from the same species but at least within the genus<sup>56–66</sup>. For each ectothermic group it was aimed that the biological process should represent the most frequent category within this group.

# Article

## Extended Data Table 2 | Source of spatial data in the terrestrial and aquatic environment

Environment (source)	GCMs/AO-GCMs	Period	Future scenarios
Terrestrial (WorldClim v2.1) <sup>49</sup>	BCC-CSM2-MR CNRM-CM6-1 CNRM-ESM2-1 CanESM5 IPSL-CM6A-LR MIROC-ES2L MIROC6 MRI-ESM2-0	2081-2100	SSP1-2.6 SSP2-4.5 SSP5-8.5
Aquatic (Bio-ORACLE v2.0) <sup>53,54</sup>	CCSM4 HadGEM2-ES MIROC5	2090-2100	RCP2.6 RCP4.5 RCP8.5

Eight General Circulation Models (GCMs) were used for the terrestrial environment and three Atmosphere–Ocean coupled GCMs (AO-GCMs) were used for the aquatic environment to build consensus models (as the average of mean and max temperature projections). Terrestrial GCMs are from the Coupled Model Intercomparison Project v6, CMIP6, while AO-GCMs are from CMIPv5. The future Shared Socioeconomic Pathways (SSP) used for terrestrial environments<sup>6</sup> are not yet available for aquatic environments, so here we used the corresponding Representative Concentration Pathways (RCPs) scenarios (RCP2.6, RCP4.5, and RCP8.5, respectively) as used in the Bio-ORACLE 2.0 database.

## Reporting Summary

Nature Portfolio wishes to improve the reproducibility of the work that we publish. This form provides structure for consistency and transparency in reporting. For further information on Nature Portfolio policies, see our [Editorial Policies](#) and the [Editorial Policy Checklist](#).

### Statistics

For all statistical analyses, confirm that the following items are present in the figure legend, table legend, main text, or Methods section.

n/a Confirmed

- The exact sample size ( $n$ ) for each experimental group/condition, given as a discrete number and unit of measurement
- A statement on whether measurements were taken from distinct samples or whether the same sample was measured repeatedly
- The statistical test(s) used AND whether they are one- or two-sided  
*Only common tests should be described solely by name; describe more complex techniques in the Methods section.*
- A description of all covariates tested
- A description of any assumptions or corrections, such as tests of normality and adjustment for multiple comparisons
- A full description of the statistical parameters including central tendency (e.g. means) or other basic estimates (e.g. regression coefficient) AND variation (e.g. standard deviation) or associated estimates of uncertainty (e.g. confidence intervals)
- For null hypothesis testing, the test statistic (e.g.  $F$ ,  $t$ ,  $r$ ) with confidence intervals, effect sizes, degrees of freedom and  $P$  value noted  
*Give  $P$  values as exact values whenever suitable.*
- For Bayesian analysis, information on the choice of priors and Markov chain Monte Carlo settings
- For hierarchical and complex designs, identification of the appropriate level for tests and full reporting of outcomes
- Estimates of effect sizes (e.g. Cohen's  $d$ , Pearson's  $r$ ), indicating how they were calculated

*Our web collection on [statistics for biologists](#) contains articles on many of the points above.*

### Software and code

Policy information about [availability of computer code](#)

Data collection Provide a description of all commercial, open source and custom code used to collect the data in this study, specifying the version used OR state that no software was used.

Data analysis R version 4.4.1

For manuscripts utilizing custom algorithms or software that are central to the research but not yet described in published literature, software must be made available to editors and reviewers. We strongly encourage code deposition in a community repository (e.g. GitHub). See the Nature Portfolio [guidelines for submitting code & software](#) for further information.

### Data

Policy information about [availability of data](#)

All manuscripts must include a [data availability statement](#). This statement should provide the following information, where applicable:

- Accession codes, unique identifiers, or web links for publicly available datasets
- A description of any restrictions on data availability
- For clinical datasets or third party data, please ensure that the statement adheres to our [policy](#)

Provide your data availability statement here.

## Human research participants

Policy information about [studies involving human research participants](#) and [Sex and Gender in Research](#).

Reporting on sex and gender

n/a

Population characteristics

n/a

Recruitment

n/a

Ethics oversight

n/a

Note that full information on the approval of the study protocol must also be provided in the manuscript.

## Field-specific reporting

Please select the one below that is the best fit for your research. If you are not sure, read the appropriate sections before making your selection.

Life sciences

Behavioural & social sciences

Ecological, evolutionary & environmental sciences

For a reference copy of the document with all sections, see [nature.com/documents/nr-reporting-summary-flat.pdf](https://nature.com/documents/nr-reporting-summary-flat.pdf)

## Ecological, evolutionary & environmental sciences study design

All studies must disclose on these points even when the disclosure is negative.

Study description

Data were collected from the litterature of heat tolerance measurements (a minimum of 3 test temperatures with corresponding heat failure times/rates per species within a single study to create a thermal death time curve) and from these data the activation energy (Ea) was calculated for each entry (species in an individual study). Here n = 123 thermal death time curves representing 112 unique species. The rate of "normal" biological processes (e.g. metabolism, enzyme rates and locomotion) at two temperatures were also collected and the activation energy was calculated, here n = 1,351 rates from 314 unique species. Activation energies of both types were then combined with climate data projections of average and maximum temperature using three different future emission scenarios, and the projected change in heat failure rates were calculated. Specific examples for two species were demonstrated by combining distribution data with local temperature (sites n=647 and 2063) and use the calculated species-specific activation energy for heat failure to indicate the percent increase in heat failure rate with climate warming.

Research sample

Data on "normal" biological rates (e.g. metabolism, enzyme rates and locomotion) measured at two temperatures were compiled from Dell et al (2011, PNAS) and Seebacher et al (2014, Nature Climate Change), and a few additional entries (n = 4, rates measured at >4 temperatures) were added as they were used in a figure. Heat failure data were collected in a litterature search, and the criterium for selection was that for a specific species heat failure time was measured at least 3 temperatures, to allow for a linear regression. Both the "normal rate" and heat failure data set includes a wide range of ectothermic species with major groups like fishes, insects, crustaceans, amphibians and molluscs represented.

Sampling strategy

No sample size calculation was performed; we collected as many entries as we could find for the heat failure data and used the available "normal" rates from Dell et al (2011, PNAS) and Seebacher et al (2014, Nature Climate Change). A few additional "normal rate" entries (n = 4, rates measured at >4 temperatures) were added as they were used in a figure.

Data collection

Heat failure data were collected in a literature search (Google Scholar) performed by LBJ, and the data found in Dell et al (2011, PNAS) and Seebacher et al (2014, Nature Climate Change) was curated to the needs of this study by LBJ. Current and projected future mean annual temperature and maximum monthly temperature was obtained for terrestrial and aquatic environments from the WorldClim v2.1 and Bio-ORACLE v2.0 databases, respectively. In these databases, current conditions represent 1970-2000 or 2000-2014 for terrestrial and aquatic environments, respectively. Future climate conditions were predicted for three future emission scenarios (SSP1-2.6, SSP2-4.5, and SSP5-8.5), from eight General Circulation Models (GCMs) for the period 2081-2100 for the terrestrial environments or three Atmosphere-Ocean coupled GCMs (AO-GCMs) for the period 2090-2100 for the aquatic environments. All climate data was used in a 5 arc minute resolution with the WGS84 datum. All climate data was analyzed and curated by MØ.

Timing and spatial scale

The litterature search was performed in the fall of 2021. The spatial scale of the climate association analysis is global.

Data exclusions

No data were excluded, except overlapping entries in the data sets from Dell et al (2011, PNAS) and Seebacher et al (2014, Nature Climate Change).

Reproducibility

Not applicable to this literature data analysis.

Randomization

Data were not randomized as only litterature data were used.

Blinding

Blinding was not used as only litterature data were used.

Did the study involve field work?  Yes  No

## Reporting for specific materials, systems and methods

We require information from authors about some types of materials, experimental systems and methods used in many studies. Here, indicate whether each material, system or method listed is relevant to your study. If you are not sure if a list item applies to your research, read the appropriate section before selecting a response.

Materials & experimental systems		Methods	
n/a	Involved in the study	n/a	Involved in the study
<input checked="" type="checkbox"/>	<input type="checkbox"/> Antibodies	<input checked="" type="checkbox"/>	<input type="checkbox"/> ChIP-seq
<input checked="" type="checkbox"/>	<input type="checkbox"/> Eukaryotic cell lines	<input checked="" type="checkbox"/>	<input type="checkbox"/> Flow cytometry
<input checked="" type="checkbox"/>	<input type="checkbox"/> Palaeontology and archaeology	<input checked="" type="checkbox"/>	<input type="checkbox"/> MRI-based neuroimaging
<input checked="" type="checkbox"/>	<input type="checkbox"/> Animals and other organisms		
<input checked="" type="checkbox"/>	<input type="checkbox"/> Clinical data		
<input checked="" type="checkbox"/>	<input type="checkbox"/> Dual use research of concern		